J Mater Sci (2007) 42:2982–2996
DOI 10.1007/s10853-006-0568-8

Reaction mechanism, kinetics and high temperature transformations of geopolymers

H. Rahier · J. Wastiels · M. Biesemans · R. Willlem · G. Van Assche · B. Van Mele

Received: 16 November 2005 / Accepted: 13 June 2006 / Published online: 12 December 2006

Abstract The reaction kinetics and mechanism of geopolymers are studied. The dissolved silicate concentration decreases from the beginning of the reaction. A characteristic time '$t_{0,vit}$' for the setting of the reaction mixture is derived from isothermal Dynamic Mechanical Analysis experiments. '$t_{0,vit}$' increases with SiO_2/R_2O but goes through a minimum for increasing water content. The reaction is slower for K compared to Na-silicate based systems. ^{29}Si and ^{27}Al solution NMR are used to probe the molecular changes. ^{27}Al NMR and FTIR reveal that an 'intermediate aluminosilicate species' (IAS) is formed from the start of the reaction. The concentration decrease of OH^- during low-temperature reaction is related to the formation of IAS. The rate law of this process seems to be obeyed by a total reaction order of 5/3, with a partial order of 1 for OH^- and 0 for Na^+ in the silicate solution. During first heating after polymerization water is lost leading to a distortion of the Al environment. According to XRD, no crystallization occurs below 900 °C. However, between 950 and 1100 °C a crystallization exotherm of nepheline is observed with DSC for a geopolymer with $SiO_2/Na_2O = 1.4$. Neither T_g of the amorphous geopolymer, nor the shrinkage and expansion around T_g during first heating, cause a measurable heat effect.

H. Rahier (✉) · G. Van Assche · B. Van Mele
Department of Physical Chemistry and Polymer Science, Vrije Universiteit Brussel, Pleinlaan 2, 1050 Brussels, Belgium
e-mail: hrahier@vub.ac.be

J. Wastiels
Department of Mechanics of Materials and Constructions, Vrije Universiteit Brussel, Pleinlaan 2, 1050 Brussels, Belgium

M. Biesemans · R. Willlem
High Resolution Nuclear Magnetic Resonance Centre, Vrije Universiteit Brussel, Pleinlaan 2, 1050 Brussels, Belgium

Introduction

The reaction at ambient temperature between an alkaline silicate solution (Sil, $(R_2O)(SiO_2)_s(H_2O)_x$) and a thermally activated clay or fly ash (as for instance metakaolinite, Mk, $(Al_2O_3)(SiO_2)_2(H_2O)_{0.05}$ [1]) yields an amorphous, glassy aluminosilicate called geopolymer [1–9]. The study of the reaction stoichiometry and the structure of geopolymer lead to the following reaction equation if starting with metakaolinite [1, 3]:

$$(R_2O)(SiO_2)_s(H_2O)_x + (Al_2O_3)(SiO_2)_2(H_2O)0.05 \rightarrow (R_2O)(Al_2O_3)(SiO2)_y(H_2O)_z$$

with R = Na or K, $s = SiO_2/R_2O$, x the (unknown) amount of bound water in the silicate solution, $y = SiO_{2,total}/Al_2O_3 = (2 + s)$ and z the amount of bound water in the aluminosilicate. The approximate value of z is 0.4 if $s = 1.4$ [1].

From Magic Angle Spinning Nuclear Magnetic Resonance (MAS NMR) is known that in geopolymer, being surrounded by 4 SiO_4 groups, Al has a high degree of symmetry [1, 3]. For Si the symmetry is less: some SiOH groups are present and there is a spread in

the amount of Al surrounding the SiO_4 units. With Fourier Transform Infrared (FTIR) a broad absorption is seen centered at 3400 cm^{-1} ascribed to both free and bound water. In the range 950–800 cm^{-1} only a small absorption is seen, indicating only few non-bridging oxygen atoms such as SiOH [3].

Some work to understand the mechanism behind the synthesis of geopolymer has already been done, for instance by Palomo et al. [10, 11]. Still, many details on the reaction mechanism and kinetics are unknown, such as the role of the cation (Li, Na or K). The cation influences the distribution of the species in the silicate solution, thus the amount of monomer, dimer etc. [12]. Also the deprotonation will be important for the reaction rate. In this paper, a brief introduction to the study of the reaction kinetics and mechanism will be given based on Modulated Temperature Differential Scanning Calorimetry (MTDSC) and Dynamic Mechanical Analysis (DMA) experiments and spectroscopic techniques.

The influence of the composition of the silicate solution (nature of the cation, value of s and w), temperature, and the mixing ratio Silicate solution/Metakaolinite (Sil/Mk) will be investigated. Some methods to study the reaction mechanism will be described.

The possibilities of ^{27}Al and ^{29}Si solution NMR to probe molecular changes during the low-temperature synthesis will be studied. The solid phase of the reaction mixture will be studied with FTIR. The evolution of pH will be followed during cure.

Geopolymers, being prepared at environmental temperature, have interesting characteristics for use at elevated temperatures [13, 14]. Compared to organic polymers and also to concrete, geopolymer can be used at much higher temperatures.

In previous work [2] was shown by Thermogravimetric Analysis (TGA) that water is evaporated from geopolymer during the first heating after low-temperature cure, and shrinkage of the material is observed by Thermomechanical Analysis (TMA) in this temperature region. At a higher temperature, around T_g a second shrinkage and subsequent expansion were observed. The question remains if important molecular transformations are involved in any of these processes (e.g. caused by the loss of structural water or SiOH groups) and if the low-temperature synthesized geopolymer is still totally amorphous after the thermal treatment.

In this paper, high-temperature Differential Scanning Calorimetry (DSC) will be used to study the high-temperature transformations of the model compound of geopolymer, with R = Na and s = 1.4 [1]. The high-temperature changes in its molecular structure will be studied by ^{29}Si and ^{27}Al MAS NMR, FTIR and high-temperature X-Ray Diffractometry (XRD).

Experimental

Raw materials and processing

The kaolinite used in this work was a well crystallized kaolin (KGa-1 from Source Clay Minerals Repository, University of Missouri, Columbia) with less than 2 weight% of impurities. The main impurities were 1.39% TiO_2 and 0.13% Fe_2O_3 [15]. To obtain metakaolinite (Mk), kaolinite was dehydroxylated in air at 700 °C for one hour.

For the 'model system' a sodium silicate solution, Na-Sil, with $SiO_2/R_2O = s = 1.4$ and $H_2O/R_2O = w = 10.0$ (in molar ratio) was used. For the study of the influence of w on the reaction rate, Na-Sil with s = 1.4 was used. To study the influence of s on the reaction rate, Na and K-Sil were used with w = 10. The Al/R ratio was always set to 1.

The mechanistic solution NMR study and the high temperature study were performed with Mk and K–Sil (s = 1.4 and w = 10.0). More details are described elsewhere [1–4].

For the high temperature study samples were obtained by mixing a stoichiometric ratio of silicate solution and Mk, and curing this mixture in a closed mould at room temperature for at least two days. For High Temperature DSC the geopolymer samples were cylindrical (sample mass ca. 100 mg). Samples for structural analysis by MAS NMR and FTIR were first cured and placed afterwards in a preheated furnace and kept isothermally during one hour at the desired temperature. The samples were powdered before analysis.

High Temperature XRD samples were cured and powdered before analysis.

Analytical techniques

Differential scanning calorimetry

Isothermal and non-isothermal measurements were performed on a DSC 2920 of TA Instruments, equipped with a temperature modulation MDSC™ option and a refrigerated cooling system (RCS). The purge gas was He at 25 mL/min.

The samples were mixed in small quantities (200 mg) with a spatula before placing in the sample pan. Reusable high pressure stainless steel sample pans

(Mettler) were used. The sample (about 30 mg) was heated as fast as possible (temperature jump) from 20 °C to the isothermal temperature. A period of 100 s and amplitude of 0.5 °C were chosen. Temperature calibration was done with cyclohexane and indium. The latter was also used for enthalpy calibration. Heat capacity was calibrated quasi-isothermally with water at 35 °C.

Dynamic mechanical analysis

The DMA 7 of PerkinElmer was used with a quartz expansion probe (diameter 1 mm). The purge gas was He at 50 mL/min. The applied frequency in all DMA measurements was 1 Hz. To study the reaction, the reaction mixture was poured in a cylindrical container and covered at the surface with a thin rubber seal (see ref. [2] for a complete description of this experimental set-up). The samples were placed in the preheated furnace. For calculating the onset of vitrification, $t_{o,vit}$, the time for heating the DMA sample from room temperature up to the cure temperature, is subtracted from the measured $t_{o,vit}$ using 5 °C/min as heating rate of the sample.

For the high temperature experiments rectangular samples of about $5 \times 5 \times 5$ mm were used.

Fourier transform infrared spectroscopy

IR spectra were obtained with a FTIR PerkinElmer 2000 using KBr pellets (13 mm pellets with ca. 1 mg sample/200 mg KBr). KBr and sample were mixed and ground in a Wig-L-Bug for 3 min and dried overnight at 110 °C before pressing the pellet.

For each spectrum, 20 scans with a resolution of 4 cm^{-1} were averaged.

Nuclear Magnetic Resonance Spectroscopy

^{29}Si and ^{27}Al spectra were obtained on a Bruker AC250 spectrometer operating at 49.70 MHz and 65.18 MHz for the ^{29}Si and ^{27}Al resonance frequencies, respectively. The spectrometer was interfaced with an Aspect-3000 computer and equipped with a MAS broad-band probe. In the case of liquid state NMR glass tubes of 10 mm diameter were used without spinning. For solid state NMR rotors of 4 mm diameter and a spinning rate of 5 kHz were used. ^{29}Si spectra were obtained over a spectral width of 9.9 kHz (acquisition time: 0.2 s), with 1000 scans and a relaxation delay of 5 s. The ^{27}Al spectra were acquired over a spectral width of 167 kHz (acquisition time: 0.04 s), with 400 scans and a relaxation delay of 0.5 s. More details are described elsewhere [1].

To quantify the amount of Al in the NMR spectrum during low-temperature cure, a capillary containing a reference Al solution was placed in the reaction mixture inside the NMR glass tube. The area of the Al signal of the reaction mixture was referenced against the area of the Al signal of this capillary (referenced itself previously against an Al standard solution with known concentration). The integration was done between 200 and –100 ppm. The Al reference solution was prepared by dissolving aluminium nitrate in a 1 M HCl solution. The Al standard solution (1.52 M) was prepared by dissolving aluminium nitrate in a sodium hydroxide solution.

Determination of OH^- concentration during low-temperature cure

The OH^- concentration of the reaction mixture during cure was estimated by titration. After a certain reaction time at 35 °C, the reaction mixture (model compound) was diluted by adding 50 times its weight in water. For an already hardened reaction mixture, the sample was pulverised prior to dilution. The diluted reaction mixture was stirred 3 min before titration. Phenolphthalein was used as an indicator. Titration was done with a 0.067 M HCl solution.

High-temperature differential scanning calorimetry

A Netzsch high-temperature DSC 404 was used. The purge gas was Ar at 50 mL/min. The sample was placed in a Pt crucible, heated at 5 °C min^{-1} from 20 °C to 1400 °C and subsequently cooled at the same rate.

High-temperature X-Ray diffractometry

X-ray diffractograms at high-temperature were recorded on a Philips diffractometer with PW 1820 goniometer but without monochromator, equipped with a high-temperature control unit HTK10.

The powdered sample was placed on the heatable Pt filament and the following temperature program was performed. After a stabilization time of 0.5 min at each temperature, the diffractogram was recorded at 30, 600, 800, and 1000 °C. The XRD recording time was 40 min. Heating between successive temperatures took 4 min. At 1000 °C, three diffractograms were registered with intervals of 30 min.

Results and discussion

Evolution of the glass transition during low-temperature cure

The evolution of T_g and other possible transitions of the 'model system' after partial cure at 35 °C are followed with non-isothermal MDSC in cooling to sub-ambient conditions and subsequent heating (Fig. 1).

For the fresh reaction mixture T_g of Na-Sil can be detected ($T_g(0) = -50$ °C) which is not influenced by the addition of Mk. After a small conversion, T_g lowers and the transition zone broadens with reaction conversion (Fig. 1b). After about 30% of heat conversion, Tg is still visible during heating but it is immediately followed by a crystallization and subsequent melting of the formed crystals (Fig. 1c). For higher conversions, crystallisation occurs already during cooling (Fig. 1d). This behaviour is explained by the exhausting of the silicate solution. SiO_4 units are consumed and incorporated in the newly formed 'pre-geopolymer oligomers' or polymer network (see further). The dilution effect might indicate that the pre-geopolymer network is phase separated from the silicate solution: the liquid silicate gets more diluted and the lower the concentration of dissolved species, the lower T_g. When the dilution becomes large enough, water in the Na-Sil will be able to crystallise during cooling.

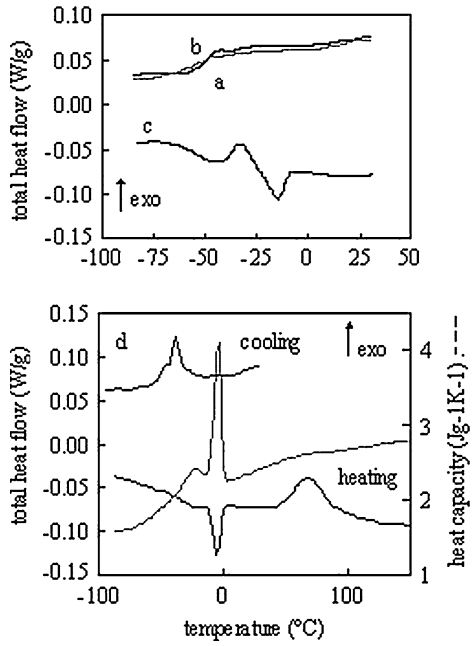

Fig. 1 Evolution of T_g and other transitions of the silicate solution (model compound) during cure at 35 °C: (**a**) cooling before cure, (**b**) cooling after 100 min cure showing broader T_g (in grey), (**c**) subsequent heating after 100 min cure, and (**d**) cooling and heating after 300 min cure including the residual reaction exotherm (total heat flow and heat capacity (in grey) curves are given)

In analogy with organic resins, one could expect T_g of the growing polymer to be somewhere between $T_g(0)$ of the silicate solution and the onset of the residual reaction exotherm: partially cured organic thermosets devitrify upon heating and restart reacting at a higher temperature [4]. For the synthesis of the geopolymer a similar decrease of the heat capacity during (isothermal) cure also occurs, indicating that T_g of the curing material reaches the isothermal cure temperature (at 35 °C this starts after ca. 100 min and 30% conversion). However, during heating after partial cure at 35 °C (Fig. 1d) no sharp increase in heat capacity as expected for devitrification is seen in a subsequent heating, even not when the reaction restarts. This is illustrated in the c_p curve of Fig. 1d: between the melting of the residual Sil (stops at ca. 0 °C) and the start of the residual exotherm no pronounced increase of c_p thus no distinct devitrification is observed. The smooth decrease in c_p during this reaction exotherm is due to further vitrification.

The residual reaction enthalpy decreases with conversion and the peak temperature of the reaction is shifted to lower temperatures at least up to a conversion of 50% (300 min) indicating the autocatalytic nature of the reaction (the peak temperature shifts from 79 °C for the fresh reaction mixture (not shown) to 69 °C in Fig. 1d).

From these results is concluded that the evolution of T_g of the growing polymer network as a function of conversion cannot be determined by MTDSC. Determination of the T_g-conversion relation is thus not straightforward for geopolymer, as opposed to most organic resins. An important difference compared to organic resins is the formation of a separate solvent (water) phase that can crystallise from a certain conversion on and in this way can create a barrier for further reaction if the material is cooled.

Quantification of rate of reaction

DMA can be used to monitor the rheological transformation during reaction [2]. In order to compare on a quantitative basis the setting or vitrification process as a function of reaction mixture compositions and reaction conditions, a reliable measure in terms of the available DMA procedure, e.g. a 'vitrification time', was defined previously [7]. The 'onset of vitrification' is defined as the time after which the storage modulus reaches an intermediate value of 10^7 Pa (Fig. 2). This value is least influenced by the

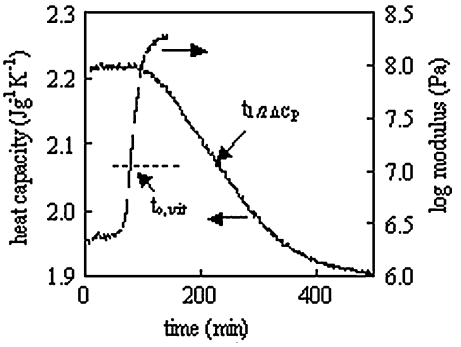

Fig. 2 DMA thermogram (storage modulus E′, retaken from[7]) and heat capacity change for the cure of the model system at 35 °C

experimental set-up and can be reproduced within an error of ±5%. The 'onset of vitrification' or '$t_{o,vit}$' is used in next sections to quantify the vitrification process of different low-temperature polymerisations.

The heat capacity signal obtained with MDSC can also be used to quantify the reaction rate. The onset of decrease in heat capacity (Fig. 2) occurs at about the same time as $t_{o,vit}$. The heat capacity signal can however be used till full conversion, whereas the storage modulus can only be measured till vitrification occurs. The time to reach half of the decrease in heat capacity, $t_{1/2\Delta c_p}$, will be used further on to compare the reactivity of different silicate solutions.

Influence of SiO_2/R_2O of the silicate solution on the reaction rate

The influence of SiO_2/R_2O or *s* on the low-temperature reaction was briefly studied with DSC in previous work [3]. A split-up and a shift of the reaction exotherm to higher temperatures, indicating a decrease of reactivity, was observed for *s* going from 1.0 to 2.3. It was also observed that the reaction exotherm of the reaction of Mk with K-Sil was shifted to higher temperatures (slower reaction) compared to Na-Sil.

The decrease of reactivity for increasing *s* is confirmed by the increase of the 'onset of vitrification' or $t_{o,vit}$ measured with DMA (Table 1). For Na-Sil, $t_{o,vit}$ is almost constant (ca. 100 min) for a value of *s* between 1.0 and 1.7, although the DSC thermogram already indicated a slower reaction for $s = 1.7$. For higher values of *s*, $t_{o,vit}$ increases fast and the reaction becomes much slower. For K-Sil compared to Na-Sil with $s = 1.4$, $t_{o,vit}$ measured at the same temperature is ca. two times longer. For these slower reactions with K-Sil, $t_{o,vit}$ was therefore measured at a higher temperature (40 °C compared to 35 °C for Na-Sil). For

Table 1 $t_{o,vit}$ as a function of s for the low-temperature reaction of Mk with Na-Sil and K-Sil

s	Na-Sil (35 °C) $t_{o,vit}$ (min) $w = 10$	K-Sil (35 °C) $t_{o,vit}$ (min)	K-Sil (40 °C) $t_{o,vit}$ (min)
0.2			57
0.8			58
1.0	98		
1.2	104		85
1.4	95	205	121
1.7	105		355
1.9	227		
2.3	484		

K-Sil at 40 °C, Table 1 further indicates that $t_{o,vit}$ increases with *s* and gets very high for $s = 1.7$.

This shows that the reaction rate is largely dependent on *s* and that the dependency seems more pronounced for K-Sil (the slower system) than for Na-Sil. It should be noted that *s* is influencing the final geopolymer structure too [3]. These results were obtained for silicate solutions with constant water content *w*. In the next section will be demonstrated that *w* has an impact on the reaction rate too.

Na-Sil with *s* between 0.0 and 0.8 were not investigated with DMA, because these silicates crystallise during cure and isothermal DMA results are falsified by this crystallisation. With DSC the isothermal reaction at 60°C of Mk with a NaOH solution (Na-Sil with $s = 0.0$) compared to a KOH solution shows a larger heat flow signal returning earlier to the baseline, again confirming that sodium solutions react faster (Fig. 3). The autocatalytic character of the reaction is best visualised in the case of the KOH solution, where the maximum reaction rate is not at the beginning of the isothermal cure but after 25 min; the sharp spike at the start is an overshoot effect.

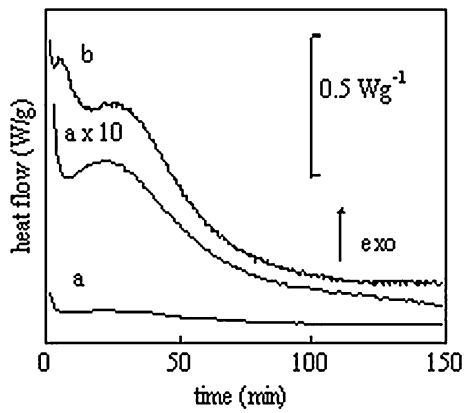

Fig. 3 DSC heat flow of isothermal cure at 60 °C of Mk with: (**a**) KOH solution and (**b**) NaOH solution

Influence of H_2O/R_2O on the low-temperature reaction rate

In previous work was shown with DSC that an increasing water content decreases the reaction rate [3, 9]. For K-Sil with different w no large differences were found in the reaction enthalpy, expressed per gram Mk. For Na-Sil, a maximum was found near the water content of model Sil ($w = 10.0$).

The 'onset of vitrification' characterised by DMA goes through a minimum (Table 2) for a value of w in the range of 8.0–10.0. The slowing down of the reaction, for low as well as for high water contents, is attributed to the decrease of concentration of reactive species. For high water contents this is evident. For decreasing water contents, the OH^- concentration increases, but at the same time the concentration of the monodeprotonated monomer $H_3SiO_4^-$ decreases in favour of the doubly deprotonated monomer [16]. Since the monodeprotonated monomer is the major reactive species for the reactions between silicate oligomers [16], it is plausible that it is also an important reactive species for the low-temperature reaction under study. So, its decreasing concentration with decreasing water content could be the reason for the decreasing reaction rate observed in Table 2.

These experiments show that the water content w is an important parameter to tune the reaction rate without significantly disturbing the final geopolymer structure [3]. Note that the value of w where the maximum rate is observed probably depends on s.

Influence of temperature on the low-temperature reaction rate

The influence of temperature on the isothermal reaction rate can also be studied by DMA (via onset of vitrification $t_{o,vit}$) and MDSC (via onset of heat capacity decrease t_{o,c_p} or half of heat capacity change $t_{1/2\Delta c_p}$ see Fig. 2). In isothermal conditions, the onset of vitrification $t_{o,vit}$ (or t_{0,c_p} and $t_{1/2\Delta c_p}$) can be considered as a point on the reaction path of constant conversion (the constant conversion level at $t_{1/2\Delta cp}$ is of course higher than at t_{o,c_p}). So, a measure for the overall reaction rate in isothermal conditions at a constant conversion and thus also for the overall rate constant, is given by the reciprocal onset of vitrification $1/t_{o,vit}$ (or $1/t_{o,c_p}$ and $t_{1/2\Delta c_p}$).

For different isothermal reactions of Mk with Na-Sil and with K-Sil, the plot of $\ln(1/t_{o,vit})$ versus the reciprocal isothermal temperature $1/T_{iso}$ shows an almost linear relation in the temperature range from 25 °C to 55 °C (Fig. 4). These graphs can be considered as a first attempt towards Arrhenius plots for the overall low-temperature production of geopolymer. An overall activation energy for the hardening process of the Na-system of ca. 84 kJ/mole can be calculated (this is a sum of several reaction steps). It is observed that the reaction is slower for the K-system, but with almost the same activation energy (75 kJ/mole).

One should be extremely careful with the interpretation of these results because of the (experimentally) limited temperature interval of the 'Arrhenius plot', the experimental errors and corrections, and the assumptions made. Indeed, the conversion at which a storage modulus of 10^7 Pa is reached (definition of $t_{o,vit}$) is also expected to increase with temperature. As a consequence, $t_{o,vit}$ values at different conversions will be compared in the same plot and the activation energy of the reaction will probably be underestimated. The activation energy of 84 kJ/mole for the 'model system' should be considered as a guide value for the low-temperature reaction.

A comparable 'Arrhenius plot' $\ln(1/t_{1/2\Delta c_p})$ versus $1/T_{iso}$ based on MDSC results is given for the model system. This MDSC plot is not coinciding with the DMA plot due to a higher conversion level at $t_1/2\Delta c_p$

Table 2 $t_{o,vit}$ as a function of w for the low-temperature reaction of Mk with Na-Sil

s	w	Na-Sil (35 °C) $t_{o,vit}$ (min) $s = 1.4$
1.4	6.6	125
1.4	8.1	100
1.4	10	95
1.4	12.2	200

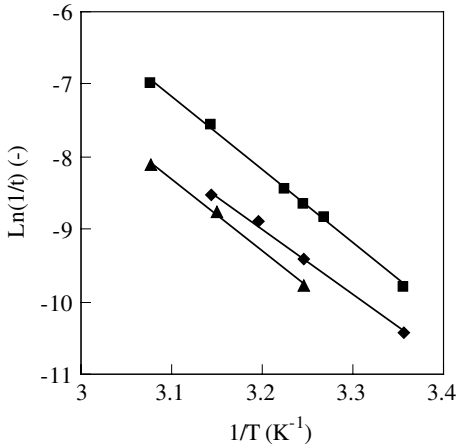

Fig. 4 $\ln(1/t_{o,vit})$ versus $1/T_{iso}$ for the 'model Na-system' (■) and for K-Sil (♦) with $s = 1.4$; $t_{o,vit}$ is measured with DMA. The lines are the 'Arrhenius plots' for corrected values of $t_{o,vit}$. $\ln(1/t_1/2\Delta c_p)$ versus $1/T_{iso}$ for the 'model Na-system' is given for comparison (▲); $t_{1/2\Delta c_p}$ is measured with MDSC

than at $t_{o,vit}$. A comparable value of 82 kJ/mole, however, is found for the activation energy.

The information of Fig. 4 is valuable for the construction of the 'vitrification line' in a time-temperature-transformation (TTT) diagram as for organic thermosets, by determining the time needed for vitrification at a chosen isothermal temperature [17].

Reaction mechanism of the low-temperature synthesis

Up to now, several conclusions about the reaction mechanism can be summarised. An important aspect of the reaction mechanism, noticed several times, is the autocatalytic character of the low-temperature reaction. This phenomenon is observed to depend on *s*, the cation, the particle size of Mk [7], and Sil/Mk. Knowledge of the reaction mechanism will help in doing kinetic modelling and thus a better control of the production process. Some initial work on mechanistic modelling, using stepwise reaction processes can be found in literature [18]. The authors also make use of autocatalytic process to simulate the heat flow signal of the reaction.

The study of the glass transition of Sil indicates that from the start of the reaction a decrease of the concentration of Sil is observed and a separate phase is growing.

Comparing the molecular structure of reactants (Sil and Mk) and geopolymer, a complete rearrangement of the molecular environment (chemical short range order SRO) of Al and Si from Mk is evident. It was shown previously [3] that Al is transformed from a distorted SRO with possibly Al^{IV}, Al^{V} and Al^{VI} and linked to one SiO_4 unit (in Mk) into a regular Al^{IV} environment surrounded by four SiO_4 units (in geopolymer). For SiO_4 units from both Mk and Sil, the amount of Al linked to the unit increases. So, the structure of Mk has to be broken down and it was observed that this reaction is rate determining for large particles [7].

More information on the reaction mechanism will be obtained via techniques that give direct molecular information or concentrations of constituents (NMR, FTIR, pH).

Mechanistic information obtained with solution NMR

The study of molecular rearrangements during cure with NMR is not straightforward because of the nature of the reaction mixture (aqueous high alkaline suspension) and the fact that it is solidifying. ^{29}Si solution NMR was already used in literature to study the liquid phase during initial stages of the reaction [9]. However, the technique suffers from the long time needed to record a spectrum (about 30 min) if one aims to get complete relaxation of the nuclei in order to be able to quantify the data. Due to the high and increasing viscosity severe peak broadening is obscuring the fine structure in the pure silicate even from the start of the reaction in the first spectrum. In the spectra of the reaction mixture, no clear evidence for new aluminosilicate species in solution is found, at least not in sufficient quantity to be detected. For these reasons non of these spectra are shown.

In the course of the reaction, a broad peak of solid material is growing under the solution peaks (^{29}Si solution NMR), covering a range from –60 to at least –120 ppm. Together with the broadening of the solution peaks, this makes accurate quantitative description of the (relative) amount of the different Q units impossible. At best one can conclude that: (i) the total concentration of Si in solution decreases at the expense of the growing polymer, and (ii) the Q units distribution tends to lower cross-link density [19]. According to literature this shift is expected from the decreasing Si concentration [20].

Although Al, in contrast to Si, is not in solution at the beginning of the reaction (only Mk contains Al), valuable information on the reaction mechanism is gained by conventional solution ^{27}Al NMR. The acquisition of ^{27}Al NMR spectra compared to ^{29}Si NMR spectra goes much faster (typically 4 min), so changes during reaction can be followed more easily.

Subsequent spectra during reaction at 40 °C are shown in Fig. 5. From the first spectrum, ca. 15 min after mixing the reactants, a signal at 61 ppm is detected. This signal does not correspond to Mk, which shows a very broad peak difficult to detect underneath the sharp signal. At first the intensity and area of the sharp signal increase as a function of increasing reaction time. After ca. 70 min, this peak decreases in intensity and afterwards an up-field shoulder at 57 ppm appears (difficult to see, see arrow in Fig. 5). This shoulder grows and becomes the most important peak.

It is obvious that at least two different species of Al (or Al SRO) occur during the low-temperature reaction. The last one with a peak position at 57 ppm is attributed to tetrahedral Al surrounded by four SiO_4 groups, $q^4(4Si)$ [1, 12]. This Al is also found in geopolymer (signal at 58 ppm [3]).

For the signal at 61 ppm, no definite peak assignment is possible at this moment, but it certainly represents tetrahedral Al. Uncertainties about the amount of Si attached to Al remain: a value of

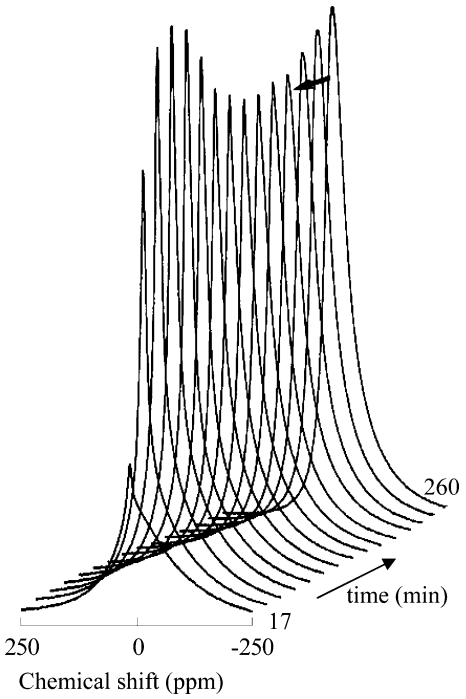

Fig. 5 Evolution of ^{27}Al NMR spectra during the reaction of Mk with K-Sil at 40 °C. The arrow indicates the appearance of the shoulder at 57 ppm

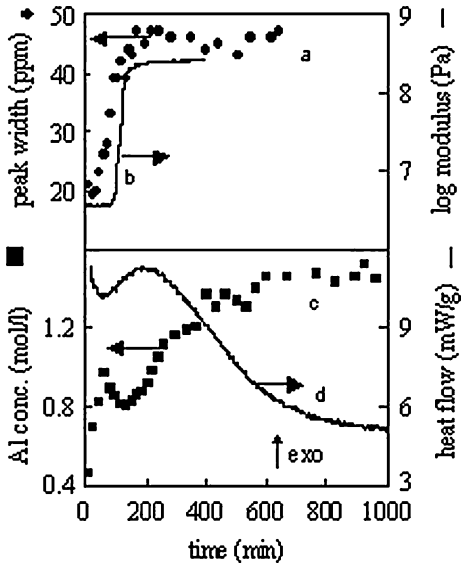

Fig. 6 Evolution during reaction of Mk with K-Sil at 40 °C of: (**a**) FWHM of total Al signal, (**b**) storage modulus (DMA), (**c**) concentration of 'detectable' Al in ^{27}Al NMR spectra; and (**d**) heat flow (DSC)

64.2 ppm was reported for q^3(3Si) species [21]. However, in analogy with the signal at 57 ppm, the signal at 61 ppm might be dissolved q^4(4Si) too. The peak width (FWHM) at 61 ppm is smaller than at 57 ppm, meaning that the Al nuclei are in a more mobile and/or less distorted environment at the start of the reaction. FWHM is still too broad, however, for being considered as a real solution state signal. This Al SRO at 61 ppm is only an intermediate species that is finally converted into q^4(4Si) in geopolymer.

If FWHM of both Al signals together is plotted as a function of time at 40 °C (Fig. 6a) and compared with the storage modulus measured with DMA in the same reaction conditions (Fig. 6b), the resemblance is obvious, especially after $t_{o,vit}$. The value of $t_{o,vit}$ (ca. 160 min) coincides with the sharp increase in FWHM.

The concentration of 'detectable' Al nuclei (total area of both peaks) seems to reach a local maximum and increases afterwards to a still higher value (Fig. 6c). FWHM reaches a minimum of 19 ppm at about the time (ca. 70 min) where the local maximum in Al concentration occurs. The final value of FWHM is 45 ppm. Whether the local maximum is significant or not might depend on the integration procedure of the Al signal. It is well known that distortion of Al sites broadens the ^{27}Al NMR signal and can even bring the signal beyond the detection limit. This leads to a decreased sensitivity for Al. This is the case for metakaolinite (therefore the signal is not detected at the beginning of the reaction), but it is also true for most glassy aluminosilicates [12] and for geopolymer. Indeed, the maximum detectable Al concentration is only 1.5 M (Fig. 6c), whereas it really is 5.8 M in the conditions of this experiment. The fact that compared to Mk, however, a relatively large and rather symmetrical Al signal at 57 ppm is seen at the end of the reaction leads to the conclusion that Al has a more symmetrical environment in geopolymer compared to Mk. Since the intermediate kind of Al (signal at 61 ppm) is more mobile than Al in geopolymer (signal at 57 ppm) it could even have a more symmetrical environment and thus a higher sensitivity. The local maximum in the total peak area could therefore be caused by a decreased sensitivity when the intermediate Al species transforms into the final form (geopolymer).

Anyhow, comparing the ^{27}Al NMR concentration profile with the DSC heat flow curve (Fig. 6d) it is striking that the local maximum in 'detectable' Al coincides with the local minimum in the heat flow curve.

The formation of the intermediate type of Al species is thus coupled to the first part of the reaction exotherm. The heat flow decreases fast here and the concentration of the intermediate type of Al species is built up fast at the same time. After ca. 70 min, the second part and autocatalytic trend becomes dominant.

From about this moment on, the network is formed and the second type of Al is perceptible and gets dominant, which is consistent with the fact that this major and final Al signal is attributed to Al in geopolymer ($q^4(4Si)$).

It is also interesting to know that the same evolution of Al spectra is observed during the reaction of Mk with a pure ROH solution, the only difference being that a minor amount of $Al(OH)_4^-$ is detected (at 79 ppm) comparable to the results from Duxson et al. [22].

In conclusion, Al from Mk seems to go through an intermediate form during reaction (probably $q^4(4Si)$), called here 'intermediate aluminosilicate species' or IAS. These intermediate species probably contribute to the main broad peaks in the solution ^{29}Si NMR spectrum [23]. They can even remain in a separate less mobile phase, e.g. micelles. They return to the solid state during further polymerisation. The reactive (or most reactive) species in Sil causing this 'dissolution' of Mk is probably OH^- and/or $H_3SiO_4^-$. From the reaction of a pure ROH solution with Mk can be concluded that OH^- is a plausible candidate. Since the rate of this latter reaction increases during an isothermal cure and the reaction rate is higher for silicate solutions, it is possible that $H_3SiO_4^-$ also plays an important role in the breakdown of Mk particles if a silicate solution is involved. For sake of simplicity, however, OH^- will be considered as the most reactive species of Sil in the further discussion of the reaction mechanism.

Based on solution ^{27}Al NMR results, a first simplified approximation of the reaction mechanism is given in following reaction scheme:

$$Mk + OH^- \rightarrow IAS \quad (1)$$

$$IAS + Sil \rightarrow geopolymer \quad (2)$$

$$IAS + IAS \rightarrow geopolymer \quad (3)$$

The intermediate aluminosilicate IAS formed in the first step is reacting further with other silicate anions or IAS species to build up geopolymer. It should be emphasised that all these steps are not to be considered as elementary reactions, but rather as complex combined reactions.

Mechanistic information obtained with FTIR

No adequate method was found to obtain good IR spectra of the reaction mixture during cure. It is however possible to investigate the solid phase in the course of the reaction after separation from the liquid phase by filtration. This is done by addition of an excess of water to the reaction mixture and subsequent filtration. The soluble products are washed out in this way and the non-soluble fraction is analysed.

Consecutive FTIR spectra of the dried solid phase show the disappearance of Mk absorptions and the formation of typical geopolymer absorptions (Fig. 7). The Si–O stretching absorption, for Mk at 1080 cm^{-1}, shifts to lower frequencies from the start of the reaction (Fig. 7b). The typical Al^{IV} absorption at 810 cm^{-1} for Mk gradually disappears, while a peak around 580 cm^{-1} and one around 700 cm^{-1} is formed. The latter peak was attributed to a coupled Si(Al)–O vibration [3].

At the start of the reaction, an important absorption at ca. 860 cm^{-1} is observed. It becomes smaller during reaction and finally only a shoulder remains. This vibration is not easily attributed. It is possible that it is caused by free $Si–O^-$ groups for example from IAS: SiO_4 groups attached to the intermediate type of Al and/or free $Si–O^-$ groups at the reactive sites of the growing polymer. It is not sure if these two types of free $Si–O^-$ groups can be distinguished, but again an intermediate is detected during reaction, probably related to IAS detected with ^{27}Al solution NMR.

Evolution of OH^- concentration during low-temperature polymerisation

For the reaction at 35 °C of model Na-Sil with Mk in stoichiometric conditions, the OH^- profile is followed by titration. Although the dilution will affect the

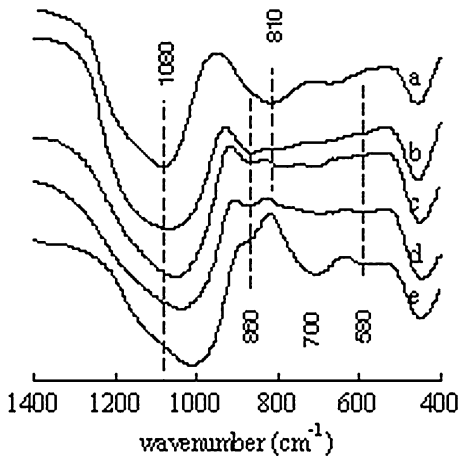

Fig. 7 IR spectra of the solid phase during cure at 40 °C ('model system'): (**a**) Mk, (**b**) after 50 min, (**c**) after 70 min, (**d**) after 100 min and (**e**) final geopolymer spectrum

speciation of the silicate species in solution, and thus the acidity, some trends can be seen and careful conclusions will be drawn from these preliminary experiments. The OH^- concentration during cure decreases quasi exponentially (Fig. 8). In comparison with the DSC heat flow signal of the same isothermal cure, the OH^- concentration follows the heat flow signal in its initial decrease, but when the heat flow gets constant or passes through a local maximum, the OH^- concentration decreases further. So, the OH^- concentration seems directly linked to the first part of the overall reaction, namely the breakdown of Mk particles and the formation of IAS. This observation is already included in the first reaction step (Eq. 1).

The decrease in OH^- concentration is in agreement with the fact that AlO_4^- units are formed during this reaction. The negative charge of each unit is supplied by OH^- and balanced by Na^+, so that the concentration of both OH^- and Na^+ should decrease. In the formation of IAS(q^4(4Si)Na^+) starting from Mk, Si from Mk(Q^4(1Al)) should be involved.

Taking into account all foregoing considerations, the following interpretation is done. The complex reaction steps (Eqs. 1–3) are written in more detail considering the Al and Si NMR SRO species involved. The species between square brackets denote species belonging to one entity (molecular or ion). In IAS the environment of Si is unknown thus it is denoted by Q?

$$\mathrm{Mk[Q^4(1Al) + Al\ SRO] + OH^- + Na^+ \rightarrow IAS[Q? + q^4(4Si)^-Na^+]} \quad (4)$$

or divided in three sub-reactions:

$$\mathrm{Mk[Q^4(1Al) + Q^4(1Al)] + OH^- \rightarrow Mk(Q^3(1Al)) + Mk(Q^3(1Al)^-)} \quad (4a)$$

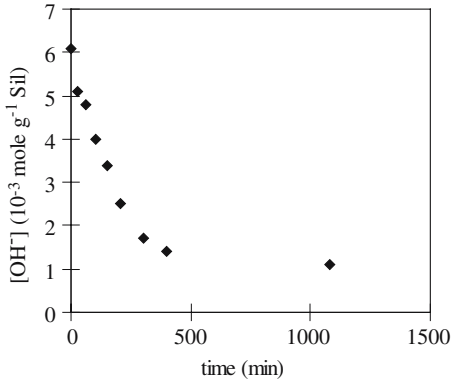

Fig. 8 OH^- concentration during cure at 35 °C (model Na-Sil)

$$\mathrm{2Mk(Al\ SRO) + OH^- \rightarrow Mk(Al\ SRO') + Mk(Al\ SRO'^-)} \quad (4b)$$

$$\mathrm{Mk(Al\ SRO') + Mk(Al\ SRO'^-) + Mk(Q3(1Al)) + Mk(Q3(1Al)^-) + 2Na^+ \rightarrow 2IAS[q^4(4Si)^-Na^+ + Q?]} \quad (4c)$$

$$\mathrm{IAS[q^4(4Si)^-Na^+ + Q?] + Sil(Q^{n-1}) \rightarrow 2\ geopolymer\ [q^4(4Si)^-Na^+ + Q^4(mAl)]} \quad (5)$$

$$\mathrm{2IAS[q^4(4Si)^-Na^+ + Q?] \rightarrow 2\ geopolymer\ [q^4(4Si)^-Na^+ + Q^4(mAl)]} \quad (6)$$

The chemical reactions in Eqs. 4a–c, 5 and 6 are the sum of elementary reactions leading to Si–O and Al–O bond breaking and Al–O–Si and Si–O–Si bond formation.

The experiment at 35 °C with OH^- titration is performed with a stoichiometric reaction mixture, according to:

$$[OH^-]_0 = [Na^+]_0 = [Al(Mk)]_0 = [Si(Mk)]_0 \cong 6 \cdot 10^{-3}\ \mathrm{mol/g\ Sil}$$

As a result, the rate law for the consumption of OH^- in Eq. 4 can be written as:

$$-\,\mathrm{d}[OH^-]/\mathrm{d}t = k_1 \cdot [OH^-]^p \quad (7)$$

with k_1 the rate constant of the reaction step in Eq. 4 and p the global reaction order. An evaluation of the global reaction order p can now be made, using the OH^- profile of Fig. 8. The best fit is obtained for $p = 1$ and $p = 5/3$. An order of 2 and more, e.g. 8/3, gives a worse correlation as seen from Fig. 9a–c. In view of reaction Equation 4 a total reaction order of 1 seems not realistic. The first reaction step (Eq. 4) is complicated by the fact that it is a liquid/solid reaction and the reaction rate is determined by the breakdown of Mk particles, depending on the specific surface of these particles. The total contact surface between liquid and solid should be incorporated in the reaction equation as a variable, decreasing with reaction conversion. Therefore, it is reasonable that the global reaction order is larger than 1, thus probably 5/3 for OH^- in Eq. 7. This total reaction order could be split up in a partial order of 1 for OH^- in Sil and a partial order of 1 for Al or Si in Mk. So, Eq. 7 can be written more explicitly as:

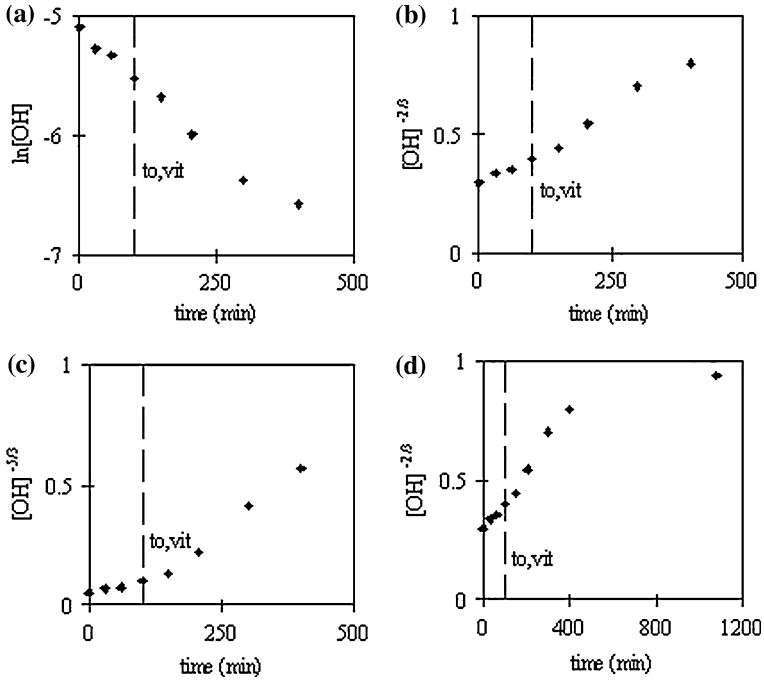

Fig. 9 Integrated rate law (Eq. 8) with global order (**a**) 1, (**b**) 5/3 and (**c**) 8/3 up to 400 min, and (**d**) global order 5/8 over the full time scale of Fig. 8. The value of $t_{o,vit}$ (DMA) is indicated for the same experimental conditions

$$-\mathrm{d}[OH^-]/\mathrm{d}t = Nk_1 \cdot [OH^-]^{5/3} = N \cdot k_1 \cdot [OH^-]^1 \cdot [OH^-]^{2/3} \quad (8)$$

with N the number of Mk particles in the reaction mixture.

The partial order of 2/3 for OH^-, would then describe the effect of Al or Si in Mk, taking into account the surface/volume ratio of a constant number N of Mk particles. Na^+ seems not to interfere in the rate law of OH^- consumption; otherwise, a global order of 8/3 would be expected and this can be excluded.

So, assuming that the formation of IAS containing the Al SRO at 61 ppm is described by the consumption of OH^-, one can conclude that the rate determining step for the dissolution process of Mk is Eq. 4a or 4b. However, care should be taken with this interpretation in view of the uncertainty of the OH^- concentration, due to the dilution effect and the fact that part of the data are obtained while the material is solidifying.

The remarkable nature of the low-temperature synthesis of geopolymer, proceeding after vitrification without diffusion control, is illustrated again in Fig. 9d. The integrated rate law for total order 5/3 (Eq. 8) is shown for the full range of the experiment (up to 1100 min or a OH^- consumption of ca. 85% at 35 °C). The rate law is obeyed up to at least 80% conversion, while only the first two measurements are performed in conditions of a liquid viscous rheology. The reaction time of the fourth measurement coincides with $t_{o,vit}$ and for all further measurements the reaction continues in the solid state. Only the measurement at 1100 min deviates from the regression line, indicating a slower reaction. The reason might be a small effect of diffusion control at the end of the isothermal reaction, and also the fact that the number N of Mk particles is no longer constant and the apparent rate constant $N \cdot k_1$ is decreasing (Eq. 8).

The autocatalytic nature of the low-temperature synthesis is also described by reaction Eqs. 4–6. Due to the 'dissolution' of Mk particles, an additional source of Q-units with cross-link density less than four is created in the course of the reaction, e.g. $Q^3(1Al)$ in Eq. 4a. As such the rate of reaction Eq. 5 for the production of geopolymer is enhanced.

It should be noted that the reaction mechanism (Eqs. 4–6) contains only the most striking information till now obtained. This preliminary mechanism is just a start for further refinement. For example the role of the monodeprotonated monomer $H_3SiO_4^-$ together with the pH dependent equilibria between mono- and doubly deprotonated monomer and all other Q-units in solution should be incorporated.

Thermal transitions of geopolymers below 900 °C

In the high-temperature DSC thermogram (Fig. 10) a large endotherm starting from the beginning of the experiment and extending to 400–600 °C is observed.

It is due to the evaporation of water and corresponds to the weight loss occurring in the same temperature interval, as measured by TGA [2]. The

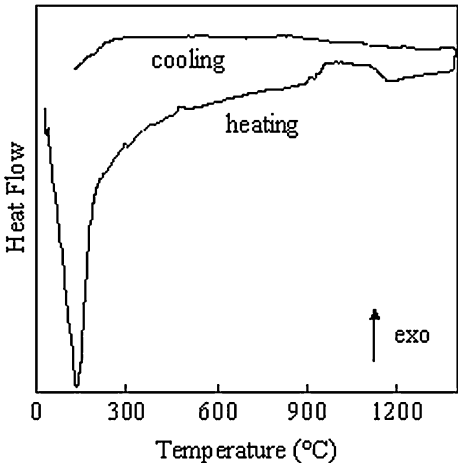

Fig. 10 High-temperature DSC thermogram (heating and cooling) of geopolymer (model system)

shape of this curve in the DSC thermogram is not only dependent on the bonding characteristics of the water to geopolymer, but also on the (cylindrical) shape of the sample. In the temperature region of the glass transition (T_g at ca. 650 °C as measured by TMA [2]), no transitions are observed in the DSC thermogram; therefore, the large shrinkage and expansion observed by TMA in the vicinity of T_g [2] occur without significant heat effect. An important conclusion is thus that T_g of geopolymer cannot be observed by DSC, which is understandable for these aluminosilicates, which are highly cross-linked networks. Due to the small structural differences below and above T_g [24], only small or negligible changes in heat capacity are to be expected. This effect is also reflected in the small increase in expansion coefficient measured by TMA [2].

The structural changes of geopolymer during the water loss are investigated by FTIR and MAS NMR. The FTIR spectra in Fig. 11 of geopolymer samples thermally treated up to 600 °C show a significant increase in the transmittance in the region of 800 cm^{-1}, compared to a sample heated at 100 °C, while the shoulder at 860 cm^{-1} disappears (compare Fig. 11a with 11b–d). This latter absorption could be due to non bridging oxygen atoms (e.g. SiOH) [3, 25, 26] and therefore it disappears upon dehydration. The OH stretching absorption at 3400 cm^{-1} (not shown), ascribed to both free and bound water [3] also vanishes during the heat treatment while the absorption band at 580 cm^{-1} decreases.

After a thermal treatment of geopolymer from 400 °C up to 800 °C, the ^{27}Al MAS NMR signal becomes skewed and broader compared to the spectrum after heating at 100 °C (Full Width at Half

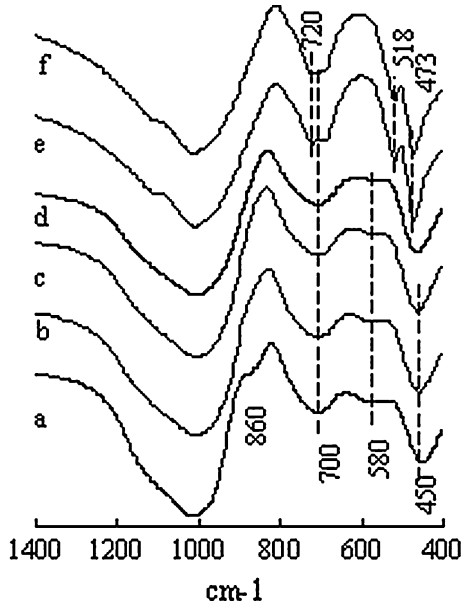

Fig. 11 Typical FTIR transmittance spectra of geopolymer after a heat treatment of 1h at: (**a**) 100 °C, (**b**) 400 °C, (**c**) 600 °C, (**d**) 700 °C, (**e**) 900 °C and (**f**) 1000 °C (model system)

Maximum (FWHM) increases from 17 to 30 ppm) while the peak position shifts from 57 to 51 ppm (compare Fig. 12a with b–c). ^{27}Al NMR reveals that

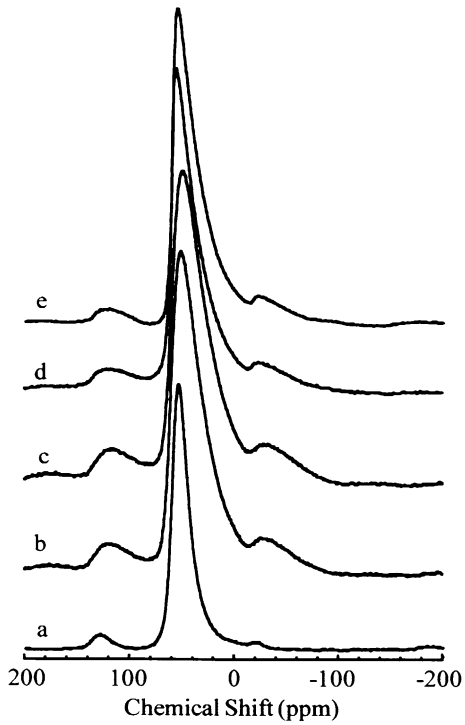

Fig. 12 Typical ^{27}Al MAS NMR spectra of geopolymer after a heat treatment of 1 h at: (**a**) 100 °C, (**b**) 400 °C, (**c**) 800 °C, (**d**) 900 °C and (**e**) 1000 °C (model system)

during the first stage of heating, below 400 °C, the short range order around Al already changes (gets more distorted), probably by an effect of water evaporation and shrinkage.

Typical ^{29}Si MAS NMR spectra of geopolymer after thermal treatment are shown in Fig. 13.

The ^{29}Si MAS NMR spectra remain almost unchanged up to 800 °C (see Fig. 13a–c). The fact that up to this temperature no significant decrease in chemical shift is observed confirms that the amount of SiOH groups in geopolymer is small (see also [1, 3]): upon heating these OH groups disappear, causing an increase in cross-link density of geopolymer. For those Si nuclei with increasing cross-link density the chemical shift should decrease by ca. 10 ppm for each additional Si–O–Si bridge [12]. Since the mean chemical shift does not change below 800 °C where, according to high-temperature DSC (Fig. 10) and TGA [2], almost all water is evaporated, the increase in cross-link density in geopolymer and so the amount of SiOH groups must be negligible.

Comparison of these results leads to the following conclusions.

Below 700 °C only IR and ^{27}Al MAS NMR reveal that structural changes occur between 100 and 400 °C. The origin of the changes could be shrinkage and a structural rearrangement due to the loss of water and OH groups, which is most important in this temperature zone (see Fig. 10b and [2]). Consequently bonds will be stressed and this can cause the broadening and peak shift of the ^{27}Al MAS NMR signal. Since the loss of water and OH groups has almost no effect on the ^{29}Si MAS NMR spectra, this result can only be understood if the amount of SiOH groups in geopolymer is small, as was already concluded in previous work [1, 3].

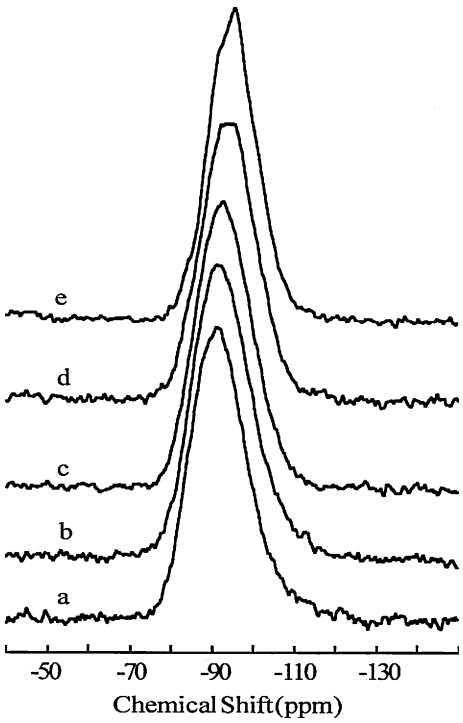

Fig. 13 Typical ^{29}Si MAS NMR spectra of geopolymer after a heat treatment of 1 h at: (**a**) 100 °C, (**b**) 400 °C, (**c**) 800 °C, (**d**) 900 °C and (**e**) 1000 °C (model system)

Thermal transitions of geopolymers above 900 °C

Between 900 and 1150 °C a broad exotherm is seen with high-temperature DSC (see Fig. 10a). No transitions are observed in the subsequent cooling or reheating up to 1400 °C.

From 900 °C on, the FTIR spectrum changes however (see Fig. 11e). A shoulder at the high frequency side of the absorption at 1000 cm^{-1} gets more pronounced. A new absorption at 720 cm^{-1} is superimposed on the peak at 700 cm^{-1}. The absorption at 450 cm^{-1} shifts to 473 cm^{-1} and gets sharper while a sharp band at 518 cm^{-1} appears. The absorptions at 473 and 518 cm^{-1} seem to indicate the appearance of a more regular structure (see later). This spectrum remains qualitatively unaltered up to the final temperature of 1400 °C (see Fig. 11f). After a thermal treatment of geopolymer from 900°C up to 1000 °C, the Al peak shifts back to ca. 55–57 ppm, becomes smaller (FWHM of 20 ppm) but stays skewed (see Fig. 12d–e). This also points to an increase of structural regularity above 800 °C.

After a thermal treatment from 900 °C up to 1000 °C, an up field Si peak shift from –91 to –96 ppm is observed (Fig. 13d–e). Since this heating is not accompanied by water loss (see earlier), this shift can no longer be caused by an increase in cross-link density and so the reason has to be sought in changing bond angles and/or lengths. After heating to 1000 °C, FWHM slightly decreases from 16 to 14 ppm and the signal consists of an even sharper peak at –96 ppm, superimposed on the broader peak. These ^{29}Si MAS NMR spectra also indicate an increase in structural regularity as already observed by ^{27}Al MAS NMR and FTIR.

Between 900 °C and 1000 °C, all spectra (FTIR, ^{27}Al and ^{29}Si MAS NMR) point in the direction of more structural regularity in the heat-treated geopolymer. This is confirmed by high-temperature XRD. The diffractograms for samples heated below 1000 °C show an amorphous bump (Fig. 14a, only one diffractogram at a temperature below 1000 °C shown, the others are comparable).

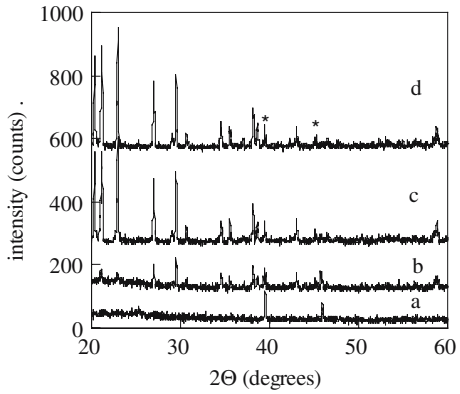

Fig. 14 High-temperature XRD spectra of geopolymer during heat treatment at (**a**) 800 °C, (**b**) 1000 °C, (**c**) 1000 °C after 70 min. and (**d**) 1000 °C after 140 min. The lines indicated with * are caused by the Pt crucible (model system)

From the first diffractogram at 1000 °C on, sharp diffraction peaks emerge. These grow with time (see Fig. 14b–d). The crystalline product is determined as nepheline ($Na_2O{\cdot}Al_2O_3{\cdot}2SiO_2$ [27]). This crystal type is known to occur in sodium aluminosilicates for glass-ceramics [28]. In glass-ceramics technology, TiO_2 is added as a nucleation catalyst. In kaolinite and Mk of this work, TiO_2 is present as an impurity and will thus accomplish the same role. So, this crystallization process seems the origin of the exothermic peak detected with high-temperature DSC (see Fig. 10).

The peak sharpening seen with Si and Al MAS NMR for samples heated to 1000 °C is also due to this crystallization process. The sharper peak in the Si MAS NMR spectrum at –96 ppm is probably caused by the nepheline phase and the broad underlying peak can then be attributed to a second Si(-rich) containing phase remaining from geopolymer.

Some IR bands of samples heated up to at least 900 °C are typical for nepheline (472 and 513 cm^{-1} [29]), but the peak at 720 cm^{-1} shows the presence of the Si-rich phase remaining from geopolymer. Indeed, comparing the compositions of 'model geopolymer' ($Na_2O{\cdot}Al_2O_3{\cdot}4SiO_2$) and nepheline ($Na_2O{\cdot}Al_2O_3{\cdot}2SiO_2$), it can be concluded that a SiO_2 phase should remain after complete segregation of nepheline. Therefore, the remaining amorphous geopolymer becomes enriched in Si during the segregation process. In the FTIR spectrum, a shift to higher frequencies is expected for this phase, probably explaining the peak at 720 cm^{-1}.

It should be noted that the necessary structural rearrangements accompanying this high-temperature crystallization process of nepheline are consistent with the bond breaking and forming mechanism in the temperature zone around and above the glass transition of geopolymer: from literature is known that T_g of inorganic polymers is defined by an equilibrium between bond breaking and formation of the same type of bonds [30, 31].

Conclusions

Vitrification of the geopolymer reaction mixture can be characterised with MDSC in both isothermal and non-isothermal experiments. The dissolved silicate concentration decreases from the beginning of the reaction, as is concluded from the decrease in T_g. T_g of the growing polymer can however not be followed directly by MDSC.

A measure for the setting time ($t_{o,vit}$: onset of vitrification) of the reaction mixture is derived from the storage modulus measured with DMA in isothermal conditions. The value of $t_{o,vit}$ increases with SiO_2/R_2O. The reaction is slower for Mk with K-Sil compared to Na-Sil. The study of the influence of the water content w shows that for Na-Sil there is a w giving rise to a maximum reaction rate. This effect needs further investigation (optimum rate for w as a function of s) because it is a way of changing the reaction rate without changing the molecular structure of geopolymer. The determination of $t_{o,vit}$ as a function of temperature gives a first indication on the overall activation energy of the low-temperature reaction.

Because of extensive peak broadening, ^{29}Si solution NMR does not give detailed information on the molecular changes during reaction. No specific dissolved aluminosilicate species are detected during cure. On the contrary, ^{27}Al solution NMR reveals the existence of two types of Al during reaction. The first type of Al species is detected immediately from the start of the reaction and is attributed to an intermediate aluminosilicate species (IAS), which is converted into the second type of Al. This latter species is finally incorporated in geopolymer together with Q-units from the silicate solution.

The OH^- concentration decreases fast and quasi exponentially at the beginning of the reaction. Comparison with heat flow and ^{27}Al solution NMR profiles leads to the conclusion that the decrease of OH^- is related to the formation of IAS and each Al is consuming one OH^- in the 'dissolution step' from Mk to IAS.

The global order of the rate law for the consumption of OH^- seems to be 5/3, with a partial order of 1 for OH^- in the silicate solution. The residual partial order of 2/3 for OH^- is describing the effect of Al or Si in Mk, taking into account the liquid/solid nature of the

reaction. A preliminary reaction model is capable of describing the effects of autocatalysis.

The thermal behaviour of geopolymer is studied by high-temperature DSC. Neither T_g itself nor the shrinkage and expansion around T_g during first heating after production of geopolymer cause a heat effect measurable by high-temperature DSC.

^{27}Al MAS NMR and FTIR spectra are influenced by the loss of structural water below 400 °C. The shrinkage and deformation accompanying water loss cause peak broadening and shift the Al NMR signal. It is remarkable that the ^{29}Si MAS NMR signal is not influenced by the loss of OH groups, but on the other hand this confirms that the amount of SiOH groups in geopolymer after low-temperature synthesis is small. The IR absorption at 860 cm^{-1} disappears upon dehydration confirming that this absorption is related to SiOH groups. According to XRD, no crystallization occurs up to 900 °C. The crystallization exotherm of a nepheline phase is observed with DSC between 950 and 1100 °C, as confirmed with high-temperature XRD and FTIR.

Acknowledgements The authors wish to thank Paul Van Oyen from the Research Development & Engineering Company REDCO of the Etex group for helpful discussions and for the high-temperature XRD measurements. Prof. Jan Van Humbeeck from the Catholic University of Leuven is thanked for the high-temperature DSC measurements.

References

1. Rahier H, Van Mele B, Biesemans M, Wastiels J, Wu X (1996) J Mater Sci 31:71
2. Rahier H, Van Mele B, Wastiels J (1996) J Mater Sci 31:80
3. Rahier H, Simons W, Van Mele B, Biesemans M (1997) J Mater Sci 32:2237
4. Van Assche G, Van Hemelrijck A, Rahier H, Van Mele B (1995) Thermochim Acta 268:121
5. Rahier H, Wullaert B, Van Mele B (2000) J Therm Anal Cal 62:417
6. Swier S, Van Assche G, Van Hemelrijck A, Rahier H, Verdonck E, Van Mele B (1998) J Thermal Anal 54:585
7. Rahier H, Denayer JF, Van Mele B (2003) J Mater Sci 38:3131
8. Duxson P, Provis JL, Lukey GC, Van Deventer JSJ, Separovic F (2005) Langmuir 21:3028
9. Barbosa VFF, Mackenzie KJD, Thaumaturgo C (2000) Int J Inorg Mater 2:309
10. Granizo ML, Blanco-Varela MT, Palomo A (2000) J Mater Sci 35:6309
11. Fernandez-Jimenez A, Palomo A, Criado M (2005) Cem Concr Res 35:1204
12. Engelhardt G, Michel D (1987) In: Engelhardt G (ed) High resolution solid state NMR of Silicates and Zeolites. J. Wiley, Chichester
13. Barbosa VFF, Mackenzie KJD (2003) Mat Res Bull 38:319
14. Barbosa VFF, Mackenzie KJD (2003) Mat Letters 57:1477
15. Van Olphen H, Fripiat JJ (1979) In: Van Olphen H (ed) Data handbook for clay materials and other non-metallic minerals. Pergamon Press, London
16. Kinrade SD, Swaddle TW (1986) J Chem Soc Chem Commun 120
17. Gillham JK, Enns JB (1994) TRIP 2(12):406
18. Provis JL, Duxson P, Van Deventer JSJ, Luckey GC (2005) Chem Eng Res Design 83:853
19. Rahier H (1995) Production, structure and properties of low-temperature synthesised inorganic polymer glasses, PhD thesis VUB, Brussels
20. Engelhardt G, Zeigan D, Jancke H, Hoebbel D, Wicker W (1975) Z Anorg Allg Chem 418:17
21. Muller D, Hoebbel D, Gessner W (1981) Chem Phys Lett 84:25
22. Duxson P, Lukey GC, Separovic F, Van Deventer JSJ (2005) Ind Eng Chem Res 44:832
23. Swaddle TW, Salerno J, Tregloan PA (1994) Chem Soc Rev 23:319
24. Turnbull D (1988) J Non-Cryst Solids 102:117
25. Roy BN (1990) J Amer Ceram Soc 73(4):846
26. Gervais F, Bln A, Massiot D, Coutures JP, Chopinet MH, Naudin F (1987) J Non-Cryst Solids 89:384
27. Macclune WF (1980) Mineral powder diffraction file. JCPDS, Swarthmore
28. Zarzycki J (1991) Glasses and the vitreous state. Cambridge University Press, Cambridge
29. Farmer VC (1974) The infrared spectra of minerals. Mineralogical society, London
30. Jewell JM, Shaw CM, Shelby JE (1993) J Non-Cryst Solids 152:32
31. Mazurin OV (1991) J Non-Cryst Solids 129:259